J. Fluid Mech. (1995), *vol.* 292, *pp.* 183–204

Adjoint systems and their role in the receptivity problem for boundary layers

By D. C. HILL†

Center for Turbulence Research, Bldg. 500, Stanford, CA 94305–3030, USA

(Received 31 August 1993 and in revised form 10 January 1995)

The effectiveness with which various sources excite convective instabilities in a boundary layer is found by a simple method. Chosen field values of the adjoint to the Tollmien–Schlichting eigensolution, normalized appropriately, indicate the amplitude of the unstable disturbance which will result for direct time-harmonic forcing by sources of momentum, mass and vorticity, as well as by boundary motions. For the Blasius boundary layer, forcing in the vicinity of the critical layer induces the largest response. At this position, the response to forcing in the wall-normal direction is typically 5% of that resulting from streamwise forcing of the same magnitude. At the wall, normal motions elicit a much stronger response than streamwise motions. Forcing close to the lower branch of the neutral stability curve leads to the largest response. The adjoint field values are equivalent to the residues of Fourier-inversion integrals. This equivalence is discussed for two problems; the vibrating ribbon problem and excitation of an inviscid free shear layer by a vorticity source. The efficiency factor is calculated for the scattering of 'acoustic' waves into Tollmien–Schlichting waves in the presence of small surface roughness, at a finite Reynolds number, based on the Orr–Sommerfeld operator. This is achieved by using the solution of an inhomogeneous adjoint problem. The results are compared with the asymptotic solutions obtained from triple-deck theory, and agree with previous finite-Reynolds-number calculations.

1. Introduction

The growth of linear Tollmien–Schlichting waves in boundary layers is of central concern in the study of transition. The many receptivity processes by which these convective instabilities are initiated play a key role in defining transition location, and are investigated by a variety of experimental and mathematical techniques.

After Schubauer & Skramstad (1947) observed Tollmien–Schlichting waves growing in a real boundary layer, Gaster (1965) modelled the response to an oscillating ribbon in terms of the spatial modes of the Orr–Sommerfeld equation. A long time after switching on the source, the flow far downstream is dominated by the spatial eigensolution with the largest streamwise growth. An analysis of forced wakes and shear layers (Huerre & Monkewitz 1985; Balsa 1988) reveals similar behaviour.

The solutions to these 'forced-response' problems emphasize the structure of the response rather than the magnitude. The amplitude of the growing wave which is produced by direct forcing depends on the nature and geometry of the source, its frequency and its physical location, together with the properties of the instability and the flow within which it exists. Such dependencies, to date, have not been charted, despite the fact that they define the physics of the process through which the unstable disturbance is established.

† Present address: Dynaflow, Inc., 3040 Riverside Drive, Suite 109, Columbus, OH 43221, USA.

The solution method is partly responsible for the lack of emphasis on this aspect of the problem. The Briggs method (Ashpis & Reshotko 1990), when applied to Fourier-inversion integrals, gives the time and space asymptotic response to a point harmonic forcing in terms of derivatives with respect to wavenumber of either a flow quantity or the dispersion relation. This is a residue from contour integration around a pole in the complex wavenumber plane (Gaster 1965; Tam 1978; Huerre & Monkwitz 1985; Balsa 1988; Ashpis & Reshotko 1990; Kozlov & Ryzhov 1990). The wavenumber derivative factors can certainly be calculated, but they retain too much mathematical complexity to provide direct understanding of the way in which the boundary layer responds to different sources and configurations.

By contrast to forced-response problems, a class of 'natural-response' problems has also been studied. Acoustic disturbances can be scattered into Tollmien–Schlichting waves by boundary roughness (Crouch 1992; Zhigulev & Fedorov 1987; Goldstein & Hultgren 1987; Goldstein 1985), by non-uniformity in the flow near a leading edge (Goldstein 1983; Goldstein, Sockol & Sanz 1983; Ackerberg & Phillips 1971), by marginal separation (Goldstein, Leib & Cowley 1987), or by mean suction or variations in surface impedance (Choudhari & Streett 1992). Here the amplitude of the response is related to the amplitude of the excitation (strength of the acoustic wave) by a coupling coefficient. This coefficient is the product of an efficiency factor, which depends upon the nature of the scattering agent, and a factor representing the geometry.

This class of problems has been addressed previously using asymptotic methods based on triple-deck theory. The solutions are constructed to be valid in the vicinity of the lower branch of the neutral stability curve, in the limit of an infinitely large Reynolds number. Solutions to natural-response problems at a finite Reynolds number are reported by Crouch (1992) and Choudhari & Streett (1992), based on the evaluation of residues. Their results indicate that the asymptotic theory provides valid estimates of the finite-Reynolds-number results, at least in the vicinity of the lower branch.

The aim of the present paper is to introduce an alternative treatment of the receptivity problem (for both forced- and natural-response classes) that features extensive use of the properties of adjoint solutions. The work of Salwen & Grosch (1981, hereinafter referred to as SG), though unrelated historically to the receptivity problem, provides a large part of the mathematical basis for the analysis. They develop a theory of temporal and spatial eigenfunction expansions for solutions of the Orr–Sommerfeld equation. The linearized Navier–Stokes equations are not self-adjoint (with respect to the usual inner product, i.e. the volume integral of the vector product of velocities), so that a bi-orthogonal eigenfunction set is required (Schensted 1960; Roberts 1960; Eckhaus 1965; Chandrasekhar 1989). For every eigensolution there is an adjoint which has an equal and opposite frequency and wavenumber, and its own distinct field. SG demonstrate that the adjoint eigensolution can be used to filter a general disturbance field to identify the amplitude of the corresponding eigensolution that is present. This is a generalization of the use of the Fourier integral to identify harmonic components.

In the present paper, properties of the bi-orthogonal eigenfunction expansion in spatial modes are used to determine the amplitude of the Tollmien–Schlichting wave component arising in both forced- and natural-response receptivity problems at a finite Reynolds number. This work provides a simple and direct means of solving both classes of problem. The concept of adjointness, which to date has been considered purely as a mathematical construct, is intimately related to the physics of the process

by which natural motions of a boundary layer are excited by external means. We investigate the form of the adjoint to the Tollmien–Schlichting wave travelling in the Blasius boundary layer, and expose aspects of the physics of that flow which have not been considered previously.

The work of SG, in which initial value problems were addressed, is extended to solve the inhomogeneous Orr–Sommerfeld problem using a modal expansion in spatial eigenmodes. The amplitude of the Tollmien–Schlichting wave, which is produced by a source distribution, is given by the inner product of the source with a particular adjoint field. The role of the adjoint eigensolutions, over and above their filtering properties, then becomes evident. The adjoint eigensolution field defines the efficiency with which a particular forcing excites the eigensolution. The amplitude of the convectively unstable eigensolution induced by harmonic point forcing is shown to be simply the value of its adjoint eigensolution at the forcing location. For momentum sources, as might be used to model a vibrating ribbon, the adjoint velocity is examined; for vorticity sources, the adjoint stream function is employed; for mass sources, the adjoint pressure is relevant. For forcing at a wall the normal adjoint stress indicates the influence of unsteady boundary motion.

At locations where the value of an adjoint eigensolution (e.g. the stream function) is large, the application of forcing (a vorticity source) will induce a large response; if the adjoint eigensolution is small, forcing at that point will elicit only a small response. This is of particular interest in problems of control, where the production of a large response with a small force is the key to effective control.

SG investigate the temporal eigenfunction expansion solution to an initial value problem and compare it to the same solution obtained by inverting a Laplace transform (Gustavsson 1979). They note that the residues and branch cut integrals are equal to the inner product of the initial field with the adjoint eigensolutions. The equivalence of the residue from contour integration and adjoint field values is discussed in the present paper for two example force-response problems which have been studied previously. For the classical vibrating ribbon problem (Ashpis & Reshotko 1990), the response amplitude reduces to the value of the *adjoint pressure* at the wall. For the excitation of an inviscid free shear layer by a point vorticity source (Huerre & Monkewitz 1985), the *adjoint stream function* at the source location alone defines the strength of coupling between source and instability.

Tollmien–Schlichting waves in the Blasius boundary layer have been studied by numerous researchers, though the form of the adjoint eigensolution has received little attention. We solve the adjoint Orr–Sommerfeld equation here – a step which is no harder than solving the regular problem. With the application of the appropriate normalization condition, the receptivity characteristics of the spatially growing Tollmien–Schlichting wave are mapped readily as a function of Reynolds number and frequency. The disturbance, as measured by the maximum streamwise velocity fluctuation, appears to be most sensitive to forcing in the neighbourhood of the critical layer (where the real part of the disturbance phase speed matches the mean flow speed). Streamwise forcing is much more effective than forcing in the wall-normal direction. At the wall, by contrast, wall-normal motions produce a much larger response than streamwise motions.

Tollmien–Schlichting waves can grow by several orders of magnitude in the unstable region, especially at lower frequencies. This growth swamps the comparatively small variations of the adjoint fields with streamwise location. Forcing at positions close to the lower branch of the neutral stability curve thus leads to the largest boundary layer response, simply by virtue of the disturbance growth factor (Crouch 1992).

Roughness or suction at the wall beneath a boundary layer scatters free-stream disturbances very effectively. The efficiency with which this process takes place is found here by solving for a second adjoint field in addition to the adjoint to the Tollmien–Schlichting wave. This second field is the solution of a carefully formulated inhomogeneous adjoint problem. As with the adjoint eigensolution, examination of the various field values indicates the effectiveness with which various agents, such as surface roughness or suction, scatter acoustic waves into Tollmien–Schlichting waves. Comparison is made with the asymptotic theory of Goldstein (1985), and direct agreement is found with the results of Crouch (1992), and Choudhari & Streett (1992).

The paper is arranged as follows. In §2 the Lagrange identity is developed. This relation is used throughout the paper. In §3 those elements of the work of SG relevant to the present study are reviewed. In §4 the general forced response problem is solved, and in §5 the theory is applied to the Blasius boundary layer. In §6 the scattering of free-stream disturbances into Tollmien–Schlichting waves is investigated.

2. The Lagrange identity and generalized Green's theorem

The Lagrange identity (Ince 1944) and generalized Green's theorem (Morse & Feshbach 1953) are key elements of the present analysis. They are developed in this section for the linearized Navier–Stokes equations for incompressible viscous flow, linearized around a steady flow $\boldsymbol{V}(\boldsymbol{r})$. All velocities are scaled on the flow velocity at infinity U_∞, pressures on ρU_∞^2 (ρ = density), and lengths on some characteristic dimension δ. Time is scaled on δ/U_∞.

Linear velocity disturbances $\boldsymbol{v}(\boldsymbol{r}, t)$ and pressure disturbances $p(\boldsymbol{r}, t)$ upon the flow $\boldsymbol{V}(\boldsymbol{r})$ satisfy

$$\frac{\partial \boldsymbol{v}}{\partial t} + \mathbf{L}(\boldsymbol{V}; R)\,\boldsymbol{v} + \boldsymbol{\nabla} p = \mathbf{0}, \tag{1}$$

$$\boldsymbol{\nabla} \cdot \boldsymbol{v} = 0, \tag{2}$$

where the ith component of the linear operator $\mathbf{L}(\boldsymbol{V}; R)$ is

$$(\mathbf{L}(\boldsymbol{V}; R)\,\boldsymbol{v})_i = V_j \frac{\partial v_i}{\partial x_j} + v_j \frac{\partial V_i}{\partial x_j} - \frac{1}{R}\frac{\partial^2 v_i}{\partial x_j^2}. \tag{3}$$

The Reynolds number is $R = U_\infty \delta/\nu$ where ν is the kinematic viscosity.

For any pair of suitably differentiable fields $\boldsymbol{s} = (\boldsymbol{v}, p)$ and $\tilde{\boldsymbol{s}} = (\tilde{\boldsymbol{v}}, \tilde{p})$ ($(\boldsymbol{v}, p)$ does not have to satisfy (1), (2)), defined over the flow domain, the following Lagrange identity is satisfied:

$$\left[\left(\frac{\partial \boldsymbol{v}}{\partial t} + \mathbf{L}(\boldsymbol{V}; R)\,\boldsymbol{v} + \boldsymbol{\nabla} p\right) \cdot \tilde{\boldsymbol{v}} + \boldsymbol{\nabla} \cdot \boldsymbol{v}\tilde{p}\right] + \left[\boldsymbol{v} \cdot \left(\frac{\partial \tilde{\boldsymbol{v}}}{\partial t} + \tilde{\boldsymbol{L}}(\boldsymbol{V}; R)\,\tilde{\boldsymbol{v}} + \boldsymbol{\nabla}\tilde{p}\right) + p\boldsymbol{\nabla} \cdot \tilde{\boldsymbol{v}}\right]$$

$$= \frac{\partial}{\partial t}(\boldsymbol{v} \cdot \tilde{\boldsymbol{v}}) + \boldsymbol{\nabla} \cdot \boldsymbol{J}(\boldsymbol{s}, \tilde{\boldsymbol{s}}), \tag{4}$$

where $\tilde{\mathbf{L}}(\boldsymbol{V}; R)$ is the adjoint linearized Navier–Stokes operator with components

$$(\tilde{\mathbf{L}}(\boldsymbol{V}; R)\,\tilde{\boldsymbol{v}})_i = V_j \frac{\partial \tilde{v}_i}{\partial x_j} - \tilde{v}_j \frac{\partial V_j}{\partial x_i} + \frac{1}{R}\frac{\partial^2 \tilde{v}_i}{\partial x_j^2}. \tag{5}$$

The vector $\boldsymbol{J}(\boldsymbol{s}, \tilde{\boldsymbol{s}})$ is the *bilinear concomitant* with components

$$(\boldsymbol{J}(\boldsymbol{s}, \tilde{\boldsymbol{s}}))_j = v_i \tilde{\sigma}_{ij} + \sigma_{ij} \tilde{v}_i, \tag{6}$$

where
$$\sigma_{ij} = p\delta_{ij} - \frac{1}{R}\frac{\partial v_i}{\partial x_j} + V_j v_i, \tag{7}$$

$$\tilde{\sigma}_{ij} = \tilde{p}\delta_{ij} + \frac{1}{R}\frac{\partial \tilde{v}_i}{\partial x_j}. \tag{8}$$

Note that replacing $-\tilde{v}_j \partial V_j/\partial x_i$ by $V_j \partial \tilde{v}_j/\partial x_i$ in (5), and replacing $\nabla\cdot v\tilde{p}$ by $\nabla\cdot v(\tilde{p} + V\cdot\tilde{v})$ in (4) also gives a valid identity, with an additional factor $V_k \tilde{v}_k \delta_{ij}$ introduced into $\tilde{\sigma}_{ij}$ This gives an apparent correspondence with the term $V_j v_i$ appearing in the definition of σ_{ij}. For the present analysis the definitions (5) and (8) serve best.

Examining the second term in square brackets on the left-hand side of the Lagrange identity (4) we define the adjoint equations

$$\frac{\partial \tilde{\boldsymbol{v}}}{\partial t} + \tilde{\mathbf{L}}(V; R)\,\tilde{\boldsymbol{v}} + \nabla\tilde{p} = \mathbf{0}, \tag{9}$$

$$\nabla\cdot\tilde{\boldsymbol{v}} = 0. \tag{10}$$

The integral over space and time of (4) gives the generalized Green's theorem for the linearized Navier–Stokes equations.

On a historical note, the use of adjoint equations as a means of solving ordinary differential equations can be traced back to work of Lagrange in the late 18th century (see Lagrange's collected works 1867). Ince (1944) credits the use of the word 'adjoint' to Fuchs (1858), though Fuchs wrote in German. There are several textbooks which deal with adjoint equations and operators within a general mathematical framework (e.g., Coddington & Levinson 1955; Morse & Feshbach 1953; Courant & Hilbert 1962; Nayfeh 1981). In bifurcation theory adjoint eigensolutions are indispensable (Iooss & Joseph 1980), since they are a key element in the application of the Fredholm alternative – a solvability condition used widely in the construction of series expansions. This solvability condition has at the same time been used to compute the effect of non-parallelism on the linear stability of boundary layer and shear flows (Ling & Reynolds 1973; Saric & Nayfeh 1975). Hill (1992) has used this approach to study the control of the global instability of a cylinder wake. Adjoint equations also play a role in the construction of variational principles for non-conservative systems (Finlayson 1972; Chandrasekhar 1989; Vujanovic & Jones 1989). The theory of eigenfunction expansions is yet another area of application. Fourier integrals are perhaps the best known examples of an eigenfunction expansion, though there are many other possibilities (Titchmarsh 1962). A theory of eigenfunction expansions for non-self-adjoint equations (many governing equations of physics are non-self-adjoint) has also been developed (Friedman & Mishoe 1956; Schensted 1960; Roberts 1960; Eckhaus 1965; Drazin & Reid 1981), with Salwen (1979) and SG studying the eigenfunction expansions for the Orr–Sommerfeld equation. In the area of receptivity, the solvability condition has been used to construct amplitude equations which describe the interaction of free-stream and boundary-layer disturbances (Zhigulev, Sidorenko & Tumin 1980; Zhigulev & Fedorov 1987). This leads to the present work where the significance of adjoint solutions is described for a variety of receptivity problems.

3. Bi-orthogonality

3.1. *A brief review*

The reader is referred to the work of SG for a detailed discussion of the bi-orthogonality properties of both the temporal and spatial eigensolutions of the Orr–Sommerfeld equation. A brief review is given here of the points relevant to the present development.

Consider a boundary layer growing along a flat plate. The Cartesian coordinate origin is located on the plate a dimensional distance L from the leading edge, and δ is chosen as $(\nu L/U_\infty)^{1/2}$. Then $\boldsymbol{V}(\boldsymbol{r}) \approx U(y)\,\hat{\boldsymbol{x}}$, where $U(y)$ is the Blasius boundary profile.

Writing $\boldsymbol{v} = \boldsymbol{\nabla} \times (\psi(x,y,t)\,\hat{\boldsymbol{z}})$ for some stream function $\psi(x,y,t)$, $\hat{\boldsymbol{z}}$ being the unit vector normal to the plane of the flow, the governing vorticity equation is given by the z-component of the curl of (1):

$$\left(\frac{\partial}{\partial t} + U\frac{\partial}{\partial x}\right)(-\nabla^2\psi) + \frac{\mathrm{d}^2 U}{\mathrm{d}y^2}\frac{\partial \psi}{\partial x} - \frac{1}{R}\nabla^2(-\nabla^2\psi) = 0. \tag{11}$$

Similarly, writing $\tilde{\boldsymbol{v}} = \boldsymbol{\nabla} \times (\tilde{\psi}(x,y,t)\,\hat{\boldsymbol{z}})$, the adjoint equation is

$$\left(\frac{\partial}{\partial t} + U\frac{\partial}{\partial x}\right)\nabla^2\tilde{\psi} + 2\frac{\mathrm{d}U}{\mathrm{d}y}\frac{\partial^2\tilde{\psi}}{\partial x\,\partial y} + \frac{1}{R}\nabla^4\tilde{\psi} = 0. \tag{12}$$

No-slip conditions

$$\psi = \partial\psi/\partial y = 0 \quad \text{and} \quad \tilde{\psi} = \partial\tilde{\psi}/\partial y = 0 \tag{13}$$

are imposed on the plate. As $|y| \to \infty$ disturbances are required to remain bounded.

With α, $\tilde{\alpha}$ being wavenumbers, and ω, $\tilde{\omega}$ being frequencies, let

$$\psi(x,y,t) = \phi_{\alpha\omega}(y)\,\mathrm{e}^{\mathrm{i}(\alpha x - \omega t)}, \quad \tilde{\psi}(x,y,t) = \tilde{\phi}_{\tilde{\alpha}\tilde{\omega}}(y)\,\mathrm{e}^{-\mathrm{i}(\tilde{\alpha}x - \tilde{\omega}t)} \tag{14}$$

be solutions of (11) and the adjoint (12), respectively (i.e. $\phi_{\alpha\omega}(y)$ satisfies the Orr–Sommerfeld equation, and $\tilde{\phi}_{\tilde{\alpha}\tilde{\omega}}(y)$ an adjoint Orr–Sommerfeld equation). The pressure eigensolution and its adjoint

$$p(x,y,t) = p_{\alpha\omega}(y)\,\mathrm{e}^{\mathrm{i}(\alpha x - \omega t)}, \quad \tilde{p}(x,y,t) = \tilde{p}_{\tilde{\alpha}\tilde{\omega}}(y)\,\mathrm{e}^{-\mathrm{i}(\tilde{\alpha}x - \tilde{\omega}t)} \tag{15}$$

then follow.

Substituting these velocity and pressure fields into the Lagrange identity (4) (with $\boldsymbol{V}(\boldsymbol{r}) = U(y)\,\hat{\boldsymbol{x}}$), the entire left-hand side is zero, from which it can be deduced (SG; Salwen 1979) that

$$-(\omega - \tilde{\omega})\langle\phi_{\alpha\omega}, \tilde{\phi}_{\tilde{\alpha}\tilde{\omega}}\rangle + (\alpha - \tilde{\alpha})[\phi_{\alpha\omega}, \tilde{\phi}_{\tilde{\alpha}\tilde{\omega}}] = 0, \tag{16}$$

with

$$\langle\phi_{\alpha\omega}, \tilde{\phi}_{\tilde{\alpha}\tilde{\omega}}\rangle = \int_0^\infty \boldsymbol{v}\cdot\tilde{\boldsymbol{v}}\,\mathrm{d}y, \quad [\phi_{\alpha\omega}, \tilde{\phi}_{\tilde{\alpha}\tilde{\omega}}] = \int_0^\infty \hat{\boldsymbol{x}}\cdot\boldsymbol{J}((\boldsymbol{v},p),(\tilde{\boldsymbol{v}},\tilde{p}))\,\mathrm{d}y. \tag{17}$$

When considering the spatial stability problem, ω and $\tilde{\omega}$ are chosen to be real and equal. SG show that both the discrete and continuous parts of the spectrum of α coincide with the spectrum for the adjoint wavenumber $\tilde{\alpha}$.

SG construct a bi-orthogonal eigensolution set. Let $\phi_{\alpha_n\omega}(y)$, $n = 1, \ldots, N(\omega)$, represent the discrete spatial modes with wavenumbers α_n, of which there are $N(\omega)$, and $\phi^{(\nu)}_{k\omega}(y)$ the continuum mode solutions (with four branches $\nu = 1, \ldots, 4$) with wavenumbers $\alpha^{(\nu)}_k$, parameterized by $0 \leqslant k < \infty$. With $\tilde{\phi}_{\alpha_n\omega}(y)$ and $\tilde{\phi}^{(\nu)}_{k\omega}(y)$ being the corresponding adjoint solutions, then

$$[\phi_{\alpha_n\omega}, \tilde{\phi}_{\alpha_m\omega}] = \delta_{nm}, \quad n, m = 1, \ldots, N(\omega), \tag{18}$$

$$[\phi^{(\nu)}_{k\omega}, \tilde{\phi}_{\alpha_n\omega}] = [\phi_{\alpha_n\omega}, \tilde{\phi}^{(\nu)}_{k\omega}] = 0, \quad \nu = 1, \ldots, 4, \tag{19}$$

$$[\phi^{(\nu)}_{k\omega}, \tilde{\phi}^{(\mu)}_{k'\omega}] = \delta(k - k')\,\delta_{\nu\mu}, \quad \nu, \mu = 1, \ldots, 4. \tag{20}$$

It follows readily from (16) that

$$\frac{\mathrm{d}\omega}{\mathrm{d}\alpha} = \frac{[\phi_{\alpha\omega}, \tilde{\phi}_{\alpha\omega}]}{\langle \phi_{\alpha\omega}, \tilde{\phi}_{\alpha\omega} \rangle}. \tag{21}$$

(Replace ω by $\omega + \delta\omega$ and $\tilde{\omega}$ by ω in (16), make a Taylor expansion for $\alpha(\omega + \delta\omega)$, then let $\delta\omega$ approach zero.) This gives an explicit expression for the group velocity for solutions of the Orr–Sommerfeld equation. This also indicates that $\langle \phi_{\alpha\omega}, \tilde{\phi}_{\alpha\omega} \rangle$ and $[\phi_{\alpha\omega}, \tilde{\phi}_{\alpha\omega}]$ differ only by a factor of the group velocity.

There is an assumption implicit in the development of SG, namely that

$$\text{if} \quad \alpha = \tilde{\alpha} \quad \text{then} \quad [\phi_{\alpha\omega}, \tilde{\phi}_{\alpha\omega}] \neq 0. \tag{22}$$

Clearly, from (21), if the chosen solution is at a branch-point singularity with $\mathrm{d}\omega/\mathrm{d}\alpha = 0$, then $[\phi_{\alpha\omega}, \tilde{\phi}_{\alpha\omega}] = 0$ ($\langle \phi_{\alpha\omega}, \tilde{\phi}_{\alpha\omega} \rangle$ is always bounded). This violates the assumption (22), and consequently the development fails since the normalization condition $[\phi_{\alpha\omega}, \tilde{\phi}_{\alpha\omega}] = 1$ cannot be applied. Schensted (1960) discusses the developments necessary to deal with such cases.

3.2. *The adjoint fields as filters*

If $\psi(x, y)\,\mathrm{e}^{-\mathrm{i}\omega t}$ is a solution of the homogeneous equation (11), it can be expressed as a sum of spatial eigensolutions

$$\psi(x, y)\,\mathrm{e}^{-\mathrm{i}\omega t} = \sum_{n=1}^{N(\omega)} a_n\, \phi_{\alpha_n \omega}(y)\,\mathrm{e}^{\mathrm{i}(\alpha_n x - \omega t)} + \sum_{\nu=1}^{4} \int_0^\infty \mathrm{d}k\, A_k^{(\nu)}\, \phi_{k\omega}^{(\nu)}(y)\,\mathrm{e}^{\mathrm{i}(\alpha_k^{(\nu)} x - \omega t)}, \tag{23}$$

where a_n and $A_k^{(\nu)}$ are constants. If $\boldsymbol{s} = (\boldsymbol{v}, p)$ represents the velocity and pressure field for which (23) is the stream function, and $\tilde{\boldsymbol{s}}_m = (\tilde{\boldsymbol{v}}_{\alpha_m \omega}(y),\ \tilde{p}_{\alpha_m \omega}(y))\,\mathrm{e}^{-\mathrm{i}(\alpha_m x - \omega t)}$ is the adjoint to the mth discrete eigenmode then

$$\int_0^\infty \hat{\boldsymbol{x}} \cdot \boldsymbol{J}(\boldsymbol{s}, \tilde{\boldsymbol{s}}_m)\,\mathrm{d}y = \sum_{n=1}^{N(\omega)} a_n [\phi_{\alpha_n \omega}, \tilde{\phi}_{\alpha_n \omega}]\,\mathrm{e}^{\mathrm{i}(\alpha_n - \alpha_m) x} + \sum_{\nu=1}^{4} \int_0^\infty \mathrm{d}k\, A_k^{(\nu)} [\phi_{k\omega}^{(\nu)}, \tilde{\phi}_{\alpha_m \omega}]\,\mathrm{e}^{\mathrm{i}(\alpha_k^{(\nu)} - \alpha_m) x}$$
$$= a_m. \tag{24}$$

A disturbance field which satisfies the homogeneous equations can be filtered using the integral on the left-hand side of (24) to identify the amplitude of a particular mode. Replacing $\tilde{\boldsymbol{s}}_m$ by the adjoint to a continuum mode yields the corresponding amplitude $A_k^{(\nu)}$.

4. Response to a time-harmonic source distribution

In this section a general forced-response problem is solved. Sources of momenta and mass, together with an unsteady boundary condition, are prescribed. The adjoint to the downstream-growing eigenmode is then used to correlate the far-field response with the sources, by employing the Lagrange identity. The effect of sources of vorticity and boundary motions is then considered. Finally, the derivation is verified by comparison with two known solutions.

4.1. *Formulation of a general problem*

Consider a source distribution oscillating harmonically at real frequency $\omega(> 0)$, including sources of momenta of strength $\boldsymbol{q}(x, y; \omega)\,\mathrm{e}^{-\mathrm{i}\omega t}$, and mass sources

$\varphi(x,y;\omega)\,e^{-i\omega t}$. Boundary velocities $\boldsymbol{v}_b(x;\omega)\,e^{-i\omega t}$ are specified at $y=0$. The governing equations are

$$-i\omega\hat{\boldsymbol{v}}+\mathbf{L}(U\hat{\boldsymbol{x}};R)\,\hat{\boldsymbol{v}}+\nabla\hat{p}=\boldsymbol{q}(x,y;\omega), \tag{25}$$

$$\nabla\cdot\hat{\boldsymbol{v}}=\varphi(x,y;\omega), \tag{26}$$

$$\hat{\boldsymbol{v}}=\boldsymbol{v}_b(x;\omega)\quad\text{on}\quad y=0, \tag{27}$$

for some fields $\hat{\boldsymbol{v}}(x,y;\omega)$ and $\hat{p}(x,y;\omega)$. The sources are assumed to be localized, in so far as they disappear for $|x|$ larger than some value $X>0$, say.

Let the discrete spatial mode of interest have stream function $\phi_{\alpha\omega}(y)\,e^{i(\alpha x-\omega t)}$, and travel downstream with $\mathrm{Re}\,(\partial\alpha/\partial\omega)$ also positive. Typically the mode with largest value of $-\mathrm{Im}\,(\alpha(\omega))$ would be considered. The amplitude of this mode far downstream as a result of the excitation by the various sources will now be found.

4.2. *Amplitude of the response*

Returning again to the Lagrange identity (4), with $V=U(y)\,\hat{\boldsymbol{x}}$, let $\boldsymbol{s}=(\boldsymbol{v},p)=(\hat{\boldsymbol{v}},\hat{p})\,e^{-i\omega t}$ be the solution to the inhomogeneous equations (25)–(27). The fields $(\tilde{\boldsymbol{v}},\tilde{p})$ are selected as the adjoint velocity and pressure field corresponding to the mode whose amplitude in the far field we wish to determine, i.e.

$$\tilde{\boldsymbol{s}}=(\tilde{\boldsymbol{v}},\tilde{p})=(\tilde{\boldsymbol{v}}_{\alpha\omega}(y),\tilde{p}_{\alpha\omega}(y))\,e^{-i(\alpha x-\omega t)},\quad\text{where}\quad\tilde{\boldsymbol{v}}_{\alpha\omega}(y)=\left(\frac{\partial\tilde{\phi}_{\alpha\omega}}{\partial y},i\alpha\tilde{\phi}_{\alpha\omega}\right). \tag{28}$$

With these substitutions we find

$$\boldsymbol{q}(x,y;\omega)\cdot\tilde{\boldsymbol{v}}_{\alpha\omega}(y)\,e^{-i\alpha x}+\varphi(x,y;\omega)\,\tilde{p}_{\alpha\omega}(y)\,e^{-i\alpha x}=\nabla\cdot\boldsymbol{J}(\boldsymbol{s},\tilde{\boldsymbol{s}}). \tag{29}$$

Integrating over y from $y=0$ to ∞, reveals that

$$\frac{\partial}{\partial x}\left(\int_0^\infty\hat{\boldsymbol{x}}\cdot\boldsymbol{J}(\boldsymbol{s},\tilde{\boldsymbol{s}})\,dy\right)=\int_0^\infty\boldsymbol{q}(x,y;\omega)\cdot\tilde{\boldsymbol{v}}_{\alpha\omega}(y)\,e^{-i\alpha x}\,dy$$

$$+\int_0^\infty\varphi(x,y;\omega)\,\tilde{p}_{\alpha\omega}(y)\,e^{-i\alpha x}\,dy+\{\hat{\boldsymbol{y}}\cdot\boldsymbol{J}(\boldsymbol{s},\tilde{\boldsymbol{s}})\}_{y=0}. \tag{30}$$

From the definition (6)–(8) of $\boldsymbol{J}$, since $\tilde{\boldsymbol{v}}_{\alpha\omega}(0)=\boldsymbol{0}$ and $\hat{\boldsymbol{v}}(x,0;\omega)=\boldsymbol{v}_b(x;\omega)$, the y-component of $\boldsymbol{J}$ on $y=0$ is

$$\boldsymbol{v}_b(x;\omega)\cdot\tilde{\mathscr{P}}_{\alpha\omega}\,e^{-i\alpha x}, \tag{31}$$

where the vector

$$\tilde{\mathscr{P}}_{\alpha\omega}=\left(\tilde{p}_{\alpha\omega}\hat{y}+\frac{1}{R}\frac{\partial\tilde{u}_{\alpha\omega}}{\partial y}\hat{x}\right)_{y=0}. \tag{32}$$

We will call this vector the *adjoint stress*.

Equation (30) is integrated from streamwise station $x=x_1(<-X)$ to station $x=x_2(>X)$. Since these locations are outside the domain of the sources, the disturbances satisfy the homogeneous equations of motion. The disturbance field can thus be decomposed into a sum of pure spatial modes. Integrating the left-hand sides of (30), and using (24), yields

$$\left[\int_0^\infty\hat{\boldsymbol{x}}\cdot\boldsymbol{J}(\boldsymbol{s},\tilde{\boldsymbol{s}})\,dy\right]_{x_1}^{x_2}=(a^{(2)}-a^{(1)})[\phi_{\alpha\omega},\tilde{\phi}_{\alpha\omega}], \tag{33}$$

where $a^{(1)}$ and $a^{(2)}$ are the respective amplitudes of the mode $\phi_{\alpha\omega}(y)\,\mathrm{e}^{\mathrm{i}(\alpha x-\omega t)}$ at x_1 and x_2. For a normalized eigenmode it follows that

$$a^{(2)}-a^{(1)}=\int_{x_1}^{x_2}\int_0^{\infty}\boldsymbol{q}(x,y,\omega)\cdot\tilde{\boldsymbol{v}}_{\alpha\omega}(y)\,\mathrm{e}^{-\mathrm{i}\alpha x}\,\mathrm{d}y\,\mathrm{d}x + \int_{x_1}^{x_2}\int_0^{\infty}\varphi(x,y;\omega)\tilde{p}_{\alpha\omega}(y)\,\mathrm{e}^{-\mathrm{i}\alpha x}\,\mathrm{d}y\,\mathrm{d}x+\int_{x_1}^{x_2}\boldsymbol{v}_b(x;\omega)\cdot\tilde{\mathscr{S}}_{\alpha\omega}\,\mathrm{e}^{-\mathrm{i}\alpha x}\,\mathrm{d}x. \quad (34)$$

The right-hand side of these equations indicates the change in amplitude of the mode between streamwise stations $x=x_1$ and $x=x_2$. If there are no sources, then there is no change in amplitude.

For convectively unstable flows, it has long been recognized (Gaster 1965) that the sign of $\mathrm{Re}\,(\partial\alpha/\partial\omega)$ determines whether a mode is excited purely upstream or purely downstream of a source distribution. For both the boundary layer and the shear layer the mode of interest appears only downstream of any sources. If x_1 is upstream of all sources, and x_2 is downstream of all sources then we can write $a^{(1)}=0$. This gives the amplitude of the mode far downstream, $a^{(2)}$, as the sum of the integrals on the right-hand side of (34).

Each source type is weighted by a different field variable of the adjoint eigensolution. Momentum source alignment with the adjoint velocity field gives a measure of the influence which that source has in exciting the instability. For a pulsating mass source the adjoint pressure provides the correlation. With a velocity specified on the boundary, the alignment with vector $\tilde{\mathscr{S}}_{\alpha\omega}\,\mathrm{e}^{-\mathrm{i}\alpha x}$ dictates how strongly the boundary motion couples to the instability.

In each instance the streamwise integration is weighted by $\mathrm{e}^{-\mathrm{i}\alpha x}$. Since, typically, $\mathrm{e}^{\mathrm{i}\alpha x}$ grows downstream, $\mathrm{e}^{-\mathrm{i}\alpha x}$ will grow upstream. There is no surprise here since sources further upstream will have a greater contribution to the far-field disturbance amplitude; the response to such sources has convected further, and hence has grown more.

4.3. *Vorticity sources and boundary motions*

Replacing $\tilde{\boldsymbol{v}}$ by its stream-function representation allows the term involving $\boldsymbol{q}(x,y;\omega)$ in (34) to be rewritten as

$$\begin{aligned}\int_{x_1}^{x_2}\int_0^{\infty}\boldsymbol{q}(x,y;\omega)\cdot\nabla\times(\tilde{\psi}\hat{\boldsymbol{z}})\,\mathrm{d}y\,\mathrm{d}x&=\int_{x_1}^{x_2}\int_0^{\infty}\{\nabla\cdot(\tilde{\psi}\hat{\boldsymbol{z}}\times\boldsymbol{q}(x,y;\omega))+(\nabla\times\boldsymbol{q}(x,y;\omega))\cdot\hat{\boldsymbol{z}}\tilde{\psi}\}\,\mathrm{d}y\,\mathrm{d}x\\&=\int_{x_1}^{x_2}\int_0^{\infty}\Omega(x,y;\omega)\,\tilde{\phi}_{\alpha\omega}(y)\,\mathrm{e}^{-\mathrm{i}\alpha x}\,\mathrm{d}y\,\mathrm{d}x,\end{aligned} \quad (35)$$

where $\Omega(x,y;\omega)\,\mathrm{e}^{-\mathrm{i}\omega t}=\hat{\boldsymbol{z}}\cdot(\nabla\times\boldsymbol{q}(x,y;\omega))\,\mathrm{e}^{-\mathrm{i}\omega t}$ is a vorticity source distribution which would appear, for example, on the right-hand side of the vorticity equation (11). Vorticity sources in the flow are weighted by the adjoint stream function.

Rather than specify a velocity at the wall, suppose now that the wall oscillates about $y=0$ with a small velocity $\boldsymbol{v}_d(x;\omega)$. The displacement of the surface from the mean position is then $-\boldsymbol{v}_d(x;\omega)/\mathrm{i}\omega$. Linearizing the boundary condition at $y=0$, an equivalent surface velocity distribution can be constructed:

$$\boldsymbol{v}_b(x;\omega)=\boldsymbol{v}_d+\frac{\boldsymbol{v}_d}{\mathrm{i}\omega}\cdot(\nabla\boldsymbol{V})_{y=0}=\hat{\boldsymbol{x}}\left\{\boldsymbol{v}_d\cdot\hat{\boldsymbol{x}}+\frac{\boldsymbol{v}_d\cdot\hat{\boldsymbol{y}}}{\mathrm{i}\omega}\left(\frac{\mathrm{d}U}{\mathrm{d}y}\right)_{y=0}\right\}+\hat{\boldsymbol{y}}(\boldsymbol{v}_d\cdot\hat{\boldsymbol{y}}). \quad (36)$$

The factor involving $\mathrm{d}U/\mathrm{d}y$ arises because the surface is displaced into a region where there is a mean flow. Substituting into the boundary integral in (34) we find that the contribution to the amplitude is

$$\int_{x_1}^{x_2} \boldsymbol{v}_b(x;\omega)\cdot\tilde{\mathscr{P}}_{\alpha\omega}\,\mathrm{e}^{-\mathrm{i}\alpha x}\,\mathrm{d}x = \int_{x_1}^{x_2} \boldsymbol{v}_a(x;\omega)\cdot\tilde{\mathscr{P}}'_{\alpha\omega}\,\mathrm{e}^{-\mathrm{i}\alpha x}\,\mathrm{d}x, \tag{37}$$

where

$$\tilde{\mathscr{P}}'_{\alpha\omega} = \left(\left(\tilde{p}_{\alpha\omega} - \frac{\mathrm{i}}{\omega R}\frac{\mathrm{d}U}{\mathrm{d}y}\frac{\partial\tilde{u}_{\alpha\omega}}{\partial y}\right)\hat{y} + \frac{1}{R}\frac{\partial\tilde{u}_{\alpha\omega}}{\partial y}\hat{x}\right)_{y=0}. \tag{38}$$

4.4. *Verification of results*

It is now illustrated that the results derived here are in agreement with two previously solved linear receptivity problems: the vibrating ribbon problem, and excitation of a free shear layer.

The classical vibrating ribbon problem was discussed in some detail recently by Ashpis & Reshotko (1990). A vibrating ribbon is placed beneath a parallel boundary layer flow (i.e. at $y = 0$) and, after $t = 0$, it oscillates with unit velocity (scaled on U_∞)

$$\boldsymbol{v}_b(x,t) = \delta(x)\,\mathrm{e}^{-\mathrm{i}\omega t}\hat{\boldsymbol{y}}. \tag{39}$$

From (34) the amplitude of the response ($x_1 < 0$, $x_2 > 0$) is

$$\int_{x_1}^{x_2} \delta(x)\,\hat{\boldsymbol{y}}\cdot\tilde{\mathscr{P}}_{\alpha\omega}\,\mathrm{e}^{-\mathrm{i}\alpha x}\,\mathrm{d}x = \tilde{p}_{\alpha\omega}(0). \tag{40}$$

Ashpis & Reshotko's solution is

$$\frac{\mathrm{i}}{(\partial v/\partial\alpha)\,(0;\alpha,\omega)}. \tag{41}$$

The equality of (40) and (41) can be shown as follows. First the linearized equations are differentiated with respect to α, while holding ω constant. Let $\boldsymbol{s}_\alpha$ denote $(\partial u/\partial\alpha,\ \partial v/\partial\alpha,\ \partial p/\partial\alpha)\,\mathrm{e}^{\mathrm{i}(\alpha x-\omega t)}$. Substituting $\boldsymbol{s}_\alpha$ and the adjoint eigenfunction into the Lagrange identity, (4), it follows quickly that

$$-\mathrm{i}\hat{\boldsymbol{x}}\cdot\boldsymbol{J}(\boldsymbol{s},\tilde{\boldsymbol{s}}) = \frac{\partial}{\partial y}(\hat{\boldsymbol{y}}\cdot\boldsymbol{J}(\boldsymbol{s}_\alpha,\tilde{\boldsymbol{s}})). \tag{42}$$

Integrating over y from $y = 0$ to ∞, and making use of (6) and (8) in evaluating the right-hand side:

$$-\mathrm{i}[\phi_{\alpha\omega},\hat{\phi}_{\alpha\omega}] = -\frac{\partial v}{\partial\alpha}(0;\alpha,\omega)\,\tilde{p}_{\alpha\omega}(0). \tag{43}$$

For a normalized solution, with $[\phi_{\alpha\omega},\tilde{\phi}_{\alpha\omega}] = 1$, it then follows that

$$\frac{\mathrm{i}}{(\partial v/\partial\alpha)\,(0;\alpha,\omega)} = \tilde{p}_{\alpha\omega}(0), \tag{44}$$

as required.

Huerre & Monkewitz (1985) consider the response of an inviscid free shear layer ($U(y)$ defined for $-\infty < y < \infty$) to excitation by a point vorticity source positioned at $x = 0$, $y = y_0$. This appears as a source

$$\Omega(x,y,t) = \delta(x)\,\delta(y-y_0)\,\mathrm{e}^{-\mathrm{i}\omega t} \tag{45}$$

in (11), with $R\to\infty$.

From (35) the response amplitude is

$$\int_{x_1}^{x_2}\int_{-\infty}^{\infty} \delta(x)\,\delta(y-y_0)\,\tilde{\phi}_{\alpha\omega}(y)\,\mathrm{e}^{-\mathrm{i}\alpha x}\,\mathrm{d}y\,\mathrm{d}x = \tilde{\phi}_{\alpha\omega}(y_0). \tag{46}$$

For convenience a change of sign is made here in the source definition from that used by Huerre & Monkewitz. The response amplitude they compute is

$$\frac{\phi_{\alpha\omega}(y_0)}{(\alpha U(y_0)-\omega)\,(\partial D/\partial\alpha)\,(y_0;\alpha,\omega)}, \quad \text{where } D(y_0;\alpha,\omega) = \left(\phi^+_{\alpha\omega}\frac{\partial\phi^-_{\alpha\omega}}{\partial y} - \phi^-_{\alpha\omega}\frac{\partial\phi^+_{\alpha\omega}}{\partial y}\right)_{y=y_{00}}. \tag{47}$$

Here $D(y_0;\alpha,\omega)$ defines the dispersion relation, and the superscript $\pm$ denotes the eigenfunction in regions $y \geqslant y_0$ and $y \leqslant y_0$ respectively.

The equality of (46) and (47) can be shown as follows. Let s^+ and s^- represent the eigensolution in the regions $y > y_0$ and $y < y_0$ respectively, and s^+_α and s^-_α be the derivatives of those fields with respect to α. Let $\tilde{s}$ represent the corresponding eigensolution, defined for all y, of the adjoint Rayleigh equation ((12) with $R \to \infty$). It follows that

$$-\mathrm{i}\hat{x}\cdot J(s^+,\tilde{s}) = (\partial/\partial y)\,(\hat{y}\cdot J(s^+_\alpha,\tilde{s})), \quad y > y_0, \tag{48}$$

$$-\mathrm{i}\hat{x}\cdot J(s^-,\tilde{s}) = (\partial/\partial y)\,(\hat{y}\cdot J(s^-_\alpha,\tilde{s})), \quad y < y_0. \tag{49}$$

Integrating (48) from $y = y_0$ to ∞, and (49) from $y = -\infty$ to y_0 and adding gives

$$\begin{aligned} -\mathrm{i}[\phi_{\alpha\omega},\tilde{\phi}_{\alpha\omega}] &= \hat{y}\cdot(J(s^-_\alpha,\tilde{s}) - J(s^+_\alpha,\tilde{s}))_{y=y_0} \\ &= -\mathrm{i}(\alpha U(y_0)-\omega)\,\tilde{\phi}_{\alpha\omega}(y_0)\,(\partial u^-/\partial\alpha - \partial u^+/\partial\alpha)_{y=y_0} \\ &= -\mathrm{i}(\alpha U(y_0)-\omega)\frac{\tilde{\phi}_{\alpha\omega}(y_0)}{\phi_{\alpha\omega}(y_0)}\frac{\partial D}{\partial\alpha}(y_0;\alpha,\omega). \end{aligned} \tag{50}$$

It then follows, on the basis that $[\phi_{\alpha\omega},\tilde{\phi}_{\alpha\omega}] = 1$, that

$$\frac{\phi_{\alpha\omega}(y_0)}{(\alpha U(y_0)-\omega)\,(\partial D/\partial\alpha)\,(y_0;\alpha,\omega)} = \tilde{\phi}_{\alpha\omega}(y_0), \tag{51}$$

as required.

5. Receptivity characteristics of the Blasius boundary layer

The Orr–Sommerfeld equation and its adjoint are solved for the Blasius profile on a finite domain $y\in[0,y_\infty]$ using a simple Chebychev Galerkin representation for $\phi_{\alpha\omega}$ and $\tilde{\phi}_{\alpha\omega}$. No-slip conditions (13) are applied on $y = 0$ and $y = y_\infty$. The transformation $y = y_\infty(c/2)(1+\xi)/(1+c-\xi)$ maps the computational variable $\xi\in[-1,1]$ onto real space, where c is a constant (Macaraeg, Streett & Hussaini 1988). For the present computations $y_\infty = 100$, $c = 1/9$, and 84 Chebychev polynomials are used. For a given frequency $f = \omega/R$, the spatial eigenvalues are found by the companion matrix and iterative methods described by Bridges & Morris (1987). These methods are equally applicable to the adjoint equations.

The Tollmien–Schlichting wave is normalized by $\max\{|u_{\alpha\omega}(y)|;y\in[0,y_\infty]\} = 1$, and $[\phi_{\alpha\omega},\tilde{\phi}_{\alpha\omega}] = 1$ (see (17)). Bi-orthogonality between eigensolutions is also verified.

Figure 1 shows $u_{\alpha\omega}(y)$ for a spatially growing Tollmien–Schlichting wave at $f = 20\times10^{-6}$, $R = 1274$, with the wavenumber being $\alpha = 0.0895-\mathrm{i}0.00377$ at this

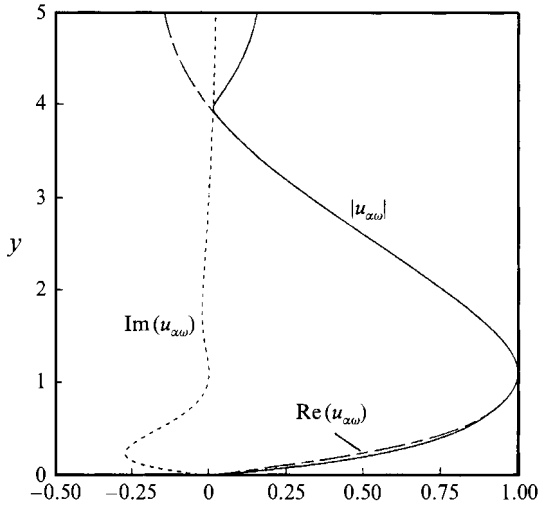

FIGURE 1. $\mathrm{Re}(u_{\alpha\omega})$, $\mathrm{Im}(u_{\alpha\omega})$, and $|u_{\alpha\omega}|$ as a function of y for a Tollmien–Schlichting wave at $f = 20 \times 10^{-6}$, $R = 1274$, $\alpha = 0.0895 - \mathrm{i}0.00377$.

condition. The maximum streamwise disturbance occurs at $y \approx 1.1$, and the disturbance persists out to, and beyond, the edge of the Blasius boundary layer (99% of free stream) at $y \approx 5$.

The corresponding adjoint streamwise velocity $\tilde{u}_{\alpha\omega}(y)$ is shown in figure 2(*a*). The maximum value of about 6.5 is taken at $y \approx 0.8$, and the field exhibits simple exponential decay beyond $y \approx 2.5$. The adjoint streamwise velocity defines the strength of Tollmien–Schlichting wave arising due to an unsteady point force aligned with the free-stream direction. A unit streamwise force applied at a height 0.8 above the wall will induce a Tollmien–Schlichting wave of amplitude 6.5. The presence of this wave will become clear further downstream when transients associated with the forcing have decayed. If the same forcing is applied further from the wall ($y > 2.5$), the response will be considerably weaker.

The simple peak structure in $|\tilde{u}_{\alpha\omega}(y)|$ is observed over a wide range of frequencies and Reynolds numbers. The maximum value taken by $|\tilde{u}_{\alpha\omega}(y)|$ and the y-location $\tilde{y}_{max}$ at which is occurs are shown in Figures 3(*a*) and 3(*b*). The frequency and Reynolds-number range are chosen to cover most of the unstable region for the Blasius boundary layer. The maximum response which can be achieved by unit-strength point streamwise forcing increases with Reynolds number. For unstable waves the distance from the wall where streamwise forcing will have the largest effect is less than 1.25. The dashed curves in figure 3(*b*) indicate the location of the critical layer (y-location such that $U(y) = \mathrm{Re}(\omega/\alpha)$). There is a clear correspondence between the location of maximum sensitivity and the critical layer.

The adjoint normal velocity $\tilde{v}_{\alpha\omega}(y)$ is shown in figure 2(*b*). This indicates how receptive the Tollmien–Schlichting wave is to point forcing aligned normal to the wall. The simple peak in $|\tilde{v}_{\alpha\omega}|$ is not as pronounced as that of $|\tilde{u}_{\alpha\omega}|$, and the magnitude of $|\tilde{v}_{\alpha\omega}|$ is significantly smaller (about 5% of $|\tilde{u}_{\alpha\omega}|$ at $y = 0.8$). Streamwise forcing will induce a much stronger response than forcing aligned normal to the wall. Note that $\tilde{\phi}_{\alpha\omega} = \mathrm{i}\alpha\tilde{v}_{\alpha\omega}$, so that the receptivity to vorticity sources is also indicated by figure 2(*b*).

The adjoint pressure $\tilde{p}_{\alpha\omega}(y)$ is shown in figure 2(*c*). This indicates how strongly a Tollmien–Schlichting wave will be excited by an unsteady point mass source, i.e. an inhomogeneity in the continuity equation. As with the adjoint velocity fields the

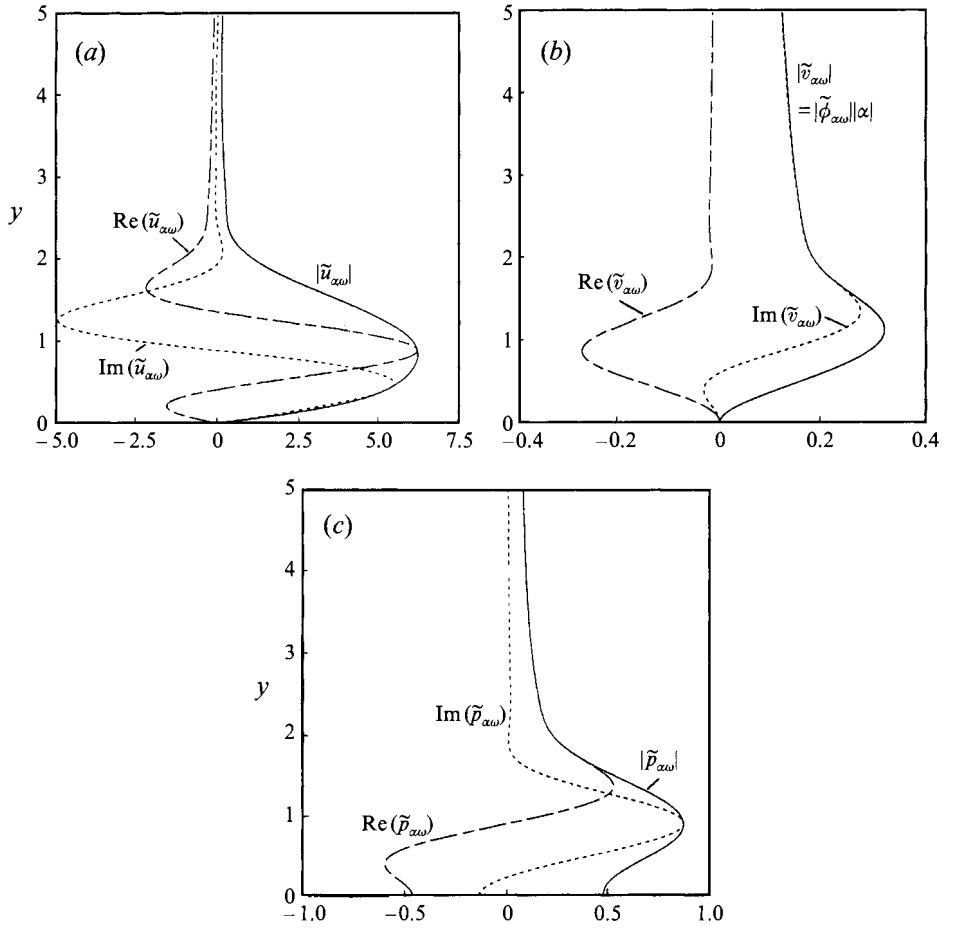

FIGURE 2. (*a*) Re($\tilde{u}_{\alpha\omega}$), Im($\tilde{u}_{\alpha\omega}$) and $|\tilde{u}_{\alpha\omega}|$; (*b*) Re($\tilde{v}_{\alpha\omega}$), Im($\tilde{v}_{\alpha\omega}$), and $|\tilde{v}_{\alpha\omega}| = |\tilde{\phi}_{\alpha\omega}||\alpha|$; (*c*) Re($\tilde{p}_{\alpha\omega}$), Im($\tilde{p}_{\alpha\omega}$), and $|\tilde{p}_{\alpha\omega}|$, all as functions of y for a Tollmien–Schlichting wave at $f = 20 \times 10^{-6}$, $R = 1274$, $\alpha = 0.0895 - i0.00377$.

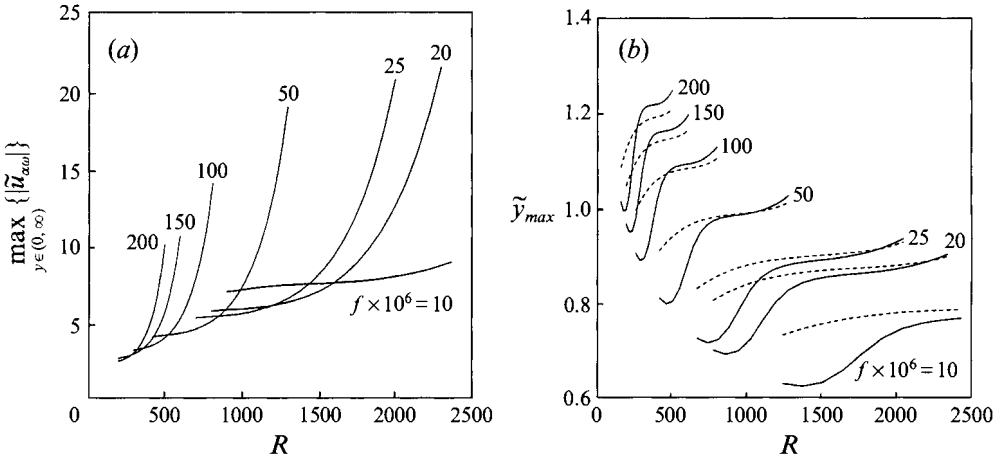

FIGURE 3. (*a*) Maximum value taken by $|\tilde{u}_{\alpha\omega}(y)|$ as a function of Reynolds number, for various frequencies. (*b*) Distance $\tilde{y}_{max}$ from the wall at which $|\tilde{u}_{\alpha\omega}(y)|$ takes its maximum value, as a function of Reynolds number, for various frequencies. Dashed lines show y_{crit}, where $U(y_{crit}) = \mathrm{Re}(\omega/\alpha)$.

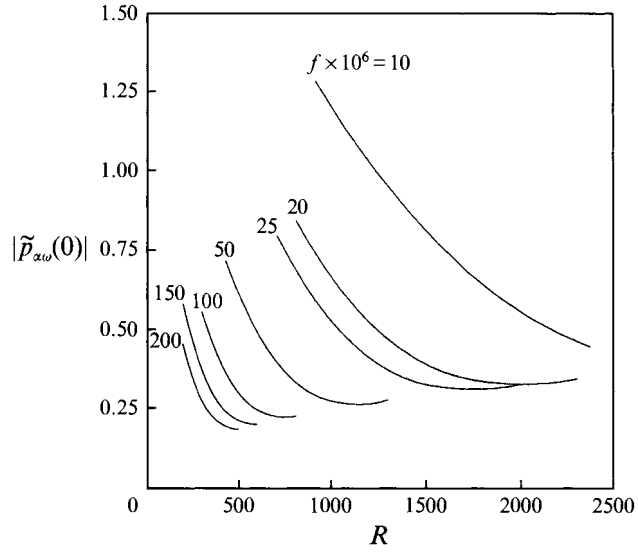

FIGURE 4. The magnitude of the adjoint pressure as the wall $|\tilde{p}_{\alpha\omega}(0)|$ as a function of Reynolds number, for various frequencies.

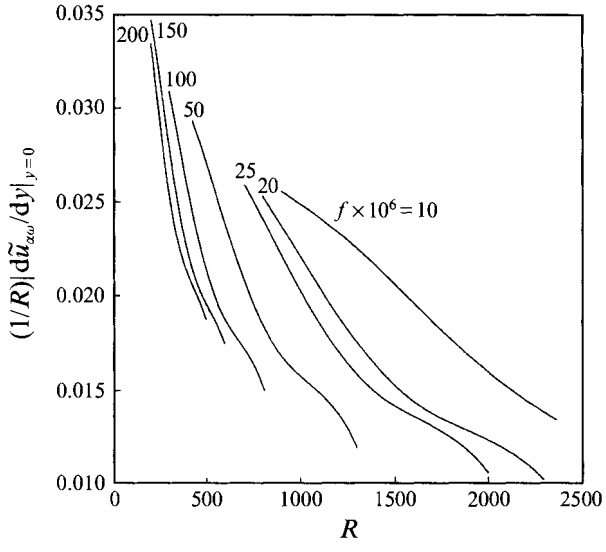

FIGURE 5. The magnitude of the adjoint wall shear $(1/R)|\mathrm{d}\tilde{u}_{\alpha\omega}/\mathrm{d}y(0)|$ as a function of Reynolds number, for various frequencies.

magnitude $|\tilde{p}_{\alpha\omega}(y)|$ has a single peak in the vicinity of $y = 1$ and decays as $y \to \infty$. The magnitude of the adjoint pressure at the wall $|\tilde{p}_{\alpha\omega}(0)|$ is shown for a range of Reynolds numbers and frequencies in figure 4. This shows how strong the response will be if there is an unsteady normal velocity at a point on the wall. The trend is one of decreasing magnitude with increasing Reynolds number until a minimum is reached in the vicinity of the upper branch.

The adjoint pressure at the wall is the normal component of the adjoint stress vector (32). The magnitude of the streamwise component, $(1/R)(\mathrm{d}u_{\alpha\omega}/\mathrm{d}y)$ evaluated at $y = 0$, is shown in figure 5. This shows how strongly the Tollmien–Schlichting wave is excited

by a streamwise velocity component at a point on the surface. Clearly, by comparison of the magnitudes in figures 4 and 5, normal velocity at the boundary induce disturbances typically 20 times larger than streamwise motions.

The various adjoint fields indicate how strongly the Tollmien–Schlichting wave is excited by a point source positioned a distance L from the plate leading edge. If the source is distributed, then the Fourier transform in the streamwise direction at the local Tollmien–Schlichting wavenumber defines a geometrical factor governing the receptivity process (see (34), (35) and (37)).

As an example, consider the response to unsteady normal suction/blowing through as slot of width d in the plate, centred a distance L from the leading edge. If $v_w(x^*/d;\omega)\,\mathrm{e}^{-\mathrm{i}\omega t}$, $-\frac{1}{2} \leqslant x^*/d \leqslant \frac{1}{2}$, defines the blowing/suction distribution, with $x^* = \delta x$ being a dimensional coordinate, the response, from (34), is

$$R_d \frac{\tilde{p}_{\alpha\omega}(0)}{R} \int_{-1/2}^{1/2} v_w(x';\omega)\,\mathrm{e}^{-\mathrm{i}2\pi(d/\lambda)\,x'}\,\mathrm{d}x'. \tag{52}$$

The change of variable $x' = \delta x/d$ has been made in the Fourier transform, $R_d = U_\infty d/\nu$ is a Reynolds number based on slot width, and $\lambda = 2\pi\delta/\alpha$ is the dimensional Tollmien–Schlichting wavelength. The wavelength λ varies slowly with Reynolds number for a given frequency. The integral depends upon the source geometry, and the slow variation of d/λ makes this a slowly varying function of the streamwise location of the slot.

Expression (52) gives the amplitude of the α-wavelength component of the disturbance in the neighbourhood of the source. The factor

$$\chi(R,f) = \exp\left[-2\int_R^{R_{lb}} \mathrm{Im}\,(\alpha(R,f))\,\mathrm{d}R\right] \tag{53}$$

defines the change in amplitude between the point of application of the forcing and the lower branch of the neutral stability curve, a convenient reference point at which to compare responses. Parameter $R_{lb}(f)$ defines the Reynolds number of the lower branch at frequency f, $\mathrm{Im}\,(\alpha(R_{lb})) = 0$. If the forcing is applied downstream of the lower branch, then this factor defines an *equivalent* amplitude. It gives the amplitude of the wave that must exist at the lower branch, in the absence of any source downstream, for a wave of the required amplitude to exist at the point where the source is to be located.

The amplitude of the Tollmien–Schlichting wave at the lower branch of the neutral stability curve is given by

$$R_d \frac{\chi(R,f)}{R} |\tilde{p}_{\alpha\omega}(0)| \left| \int_{-1/2}^{1/2} v_w(x';\omega)\,\mathrm{e}^{-\mathrm{i}2\pi(d/\lambda)\,x'}\,\mathrm{d}x' \right|. \tag{54}$$

A plot of $\log_{10}(\chi(R,f)/R)$ as a function of R is shown in figure 6, for various choices of frequency f.

The factor $\chi(R,f)/R$ clearly can vary by several orders of magnitude, especially for the lower frequencies. The magnitude of the adjoint pressure, shown in figure 4, varies by less than one order of magnitude with both frequency and Reynolds number. Thus for a source of given geometry and strength, the variation of the response as a function of the streamwise position of the source will be dominated by the factor $\chi(R,f)/R$: the distance that the Tollmien–Schlichting wave is free to travel through the unstable region is the most significant factor in determining a measure of the response, especially at lower frequencies.

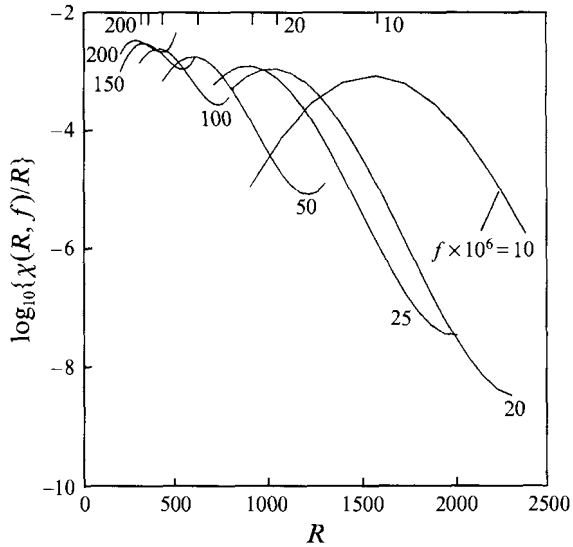

FIGURE 6. Plot of the factor $\log_{10}(\chi(R,f)/R)$ as a function of Reynolds number, for various frequencies. The lower-branch position at each frequency is indicated by the ticks at the top of the figure.

A similar argument follows for the response to a vibrating ribbon, which can be modelled as an unsteady source of momentum in the flow. Examination of the adjoint velocity field indicates that, at a distance L from the leading edge, positioning the ribbon in the vicinity of $y = 0.8$ (a physical height 0.8 $(\nu L/U_\infty)^{1/2}$ above the plate, or about half the displacement thickness) will lead to the largest response. When the ribbon is located close to the lower branch (physical distance $(R_{lb}(f))^2\nu/U_\infty$ from the leading edge) the largest overall response will be achieved because the wave is able to grow most by travelling through the entire unstable region. (This is a more realistic source model than that used in the analyses of Gaster 1965 and Ashpis & Reshotko 1990. The emphasis in those analyses was, of course, on the structure rather than the magnitude of the response.)

6. Scattering of free-stream disturbances

6.1. *Surface roughness*

Sound waves in the free stream can be scattered into Tollmien–Schlichting waves in a boundary layer if the surface is rough. This scattering is believed to play a significant role in the transition process, and was investigated by Goldstein (1985) using triple-deck theory to obtain the behaviour in the infinite-Reynolds-number asymptotic limit near the lower branch of the neutral stability curve. That problem is solved here using an adjoint approach within the framework of the Orr–Sommerfeld operator. A finite-Reynolds-number approach has also been developed by Crouch (1992) and Choudhari & Streett (1992), for incompressible flow, and by Zhigulev & Fedorov (1987) for compressible flow.

Consider a flow whose velocity approaches a uniform mean flow plus small planar fluctuations $\hat{\boldsymbol{x}}\,\mathrm{e}^{-\mathrm{i}\omega t}$ in the streamwise direction as $y \to \infty$. Such a motion represents the passage of an (infinite-wavelength) acoustic wave in the free stream.

Consider a rough boundary whose mean position lies at $y = 0$, with the displacement from $y = 0$ being $\epsilon_h\, h(x)$, where $|h(x)| \leqslant 1$, and $h(x) = 0$ for $|x|$ larger than some value

X_0, say. The roughness will serve to scatter the unsteady motion far from the surface into Tollmien–Schlichting waves. We would like to correlate the amplitude of these waves with the acoustic motion. This can be achieved by performing a perturbation analysis on the basis that the roughness, as measured by ϵ_h, is sufficiently small.

In the absence of any roughness there is a profile $U(y)$ on top of which is superimposed an unsteady motion

$$\boldsymbol{v}(\boldsymbol{r}, t) = u(y)\,\mathrm{e}^{-\mathrm{i}\omega t}\,\hat{\boldsymbol{x}}, \quad \text{where} \quad u(y) = 1-\mathrm{e}^{-(\omega R/2)^{1/2}(1-\mathrm{i})\,y}. \tag{55}$$

The growth of the unperturbed boundary layer can be ignored to the present order of approximation. The planar fluctuations have a Stokes' wave signature close to the plate.

Let the roughness perturb the mean flow by $\epsilon_h \boldsymbol{S}'$, and the unsteady flow by $\epsilon_h(\boldsymbol{v}'(\boldsymbol{r}), p'(\boldsymbol{r}))\,\mathrm{e}^{-\mathrm{i}\omega t}$. Here $\boldsymbol{S}' = (\boldsymbol{V}'(\boldsymbol{r}), P'(\boldsymbol{r}))$, with $\boldsymbol{V}' = U'\hat{\boldsymbol{x}} + V'\hat{\boldsymbol{y}}$. At order ϵ_h the mean flow correction is described by

$$\mathbf{L}(U\hat{\boldsymbol{x}}; R)\,\boldsymbol{V}' + \boldsymbol{\nabla} P' = \boldsymbol{0}, \tag{56}$$

$$\boldsymbol{\nabla}\cdot\boldsymbol{V}' = 0, \tag{57}$$

$$\boldsymbol{V}' = -h(x)\frac{\mathrm{d}U}{\mathrm{d}y}\hat{\boldsymbol{x}} \quad \text{on} \quad y = 0,$$

$$\to \boldsymbol{0} \quad \text{as} \quad x \to \pm\infty,\ \forall y, \quad \text{and as} \quad y \to \infty,\ \forall x. \tag{58}$$

In fact, it is assumed that far from the roughness patch the flow field recovers sufficiently quickly that the scattering takes place in an interaction zone in the vicinity of the roughness.

For the correction to the unsteady motion (55)

$$-\mathrm{i}\omega\boldsymbol{v}' + \mathbf{L}(U\hat{\boldsymbol{x}}; R)\,\boldsymbol{v}' + \boldsymbol{\nabla} p' = -\hat{\boldsymbol{x}}\left(V'\frac{\mathrm{d}u}{\mathrm{d}y} + u\frac{\partial U'}{\partial x}\right) - \hat{\boldsymbol{y}}u\frac{\partial V'}{\partial x}, \tag{59}$$

$$\boldsymbol{\nabla}\cdot\boldsymbol{v}' = 0, \tag{60}$$

$$\boldsymbol{v}' = -h(x)\frac{\mathrm{d}u}{\mathrm{d}y}\hat{\boldsymbol{x}} \quad \text{on} \quad y = 0. \tag{61}$$

It is also required that there be no Tollmien–Schlichting wave approaching the region from upstream, at this order. The flow and boundary distortion introduce effective sources of momenta and boundary motion, which excite Tollmien–Schlichting waves. The linearization of the boundary condition requires that the surface be displaced much less than a quarter of a Stokes' wavelength, i.e. $\epsilon_h \ll (\pi^2/2\omega R)^{1/2}$.

Now consider a control volume $-X < x < X$, $0 < y < \infty$, for some $X(> X_0)$. Writing

$$a_{\pm}(X) = \int_0^{\infty} [\boldsymbol{J}((\boldsymbol{v}', p')\,\mathrm{e}^{-\mathrm{i}\omega t}, (\tilde{\boldsymbol{v}}_{\alpha\omega}, \tilde{p}_{\alpha\omega})\,\mathrm{e}^{-\mathrm{i}(\alpha x-\omega t)})\cdot\hat{\boldsymbol{x}}]_{x=\pm X}\,\mathrm{d}y, \tag{62}$$

it follows, using a similar procedure to that pursued to solve (25)–(27), that

$$a_+ - a_- = A_1 + A_2, \tag{63}$$

where A_1 and A_2 give the contributions from the momenta and wall sources respectively:

$$A_1 = -\int_{-X}^{X}\mathrm{d}x\int_0^{\infty}\mathrm{d}y\left(\tilde{u}_{\alpha\omega}\left(V'\frac{\mathrm{d}u}{\mathrm{d}y} + u\frac{\partial U'}{\partial x}\right) + \tilde{v}_{\alpha\omega}u\frac{\partial V'}{\partial x}\right)\mathrm{e}^{-\mathrm{i}\alpha x}, \tag{64}$$

$$A_2 = -\left(\frac{\mathrm{d}u}{\mathrm{d}y}\right)_{y=0}(\hat{\boldsymbol{x}}\cdot\tilde{\boldsymbol{\mathscr{F}}}_{\alpha\omega})\int_{-X}^{X}\mathrm{d}x\,h(x)\,\mathrm{e}^{-\mathrm{i}\alpha x}. \tag{65}$$

Integrating A_1 by parts:

$$A_1 = -\int_{-X}^{X} \mathrm{d}x \int_0^\infty \mathrm{d}y\, \boldsymbol{V}'(x,y)\cdot\tilde{\boldsymbol{Q}}(y)\,\mathrm{e}^{-\mathrm{i}\alpha x} + \Gamma'(X), \tag{66}$$

where

$$\tilde{\boldsymbol{Q}}(y) = \mathrm{i}\alpha u\tilde{u}_{\alpha\omega}\,\hat{\boldsymbol{x}} + \left(\mathrm{i}\alpha u\tilde{v}_{\alpha\omega} + \tilde{u}_{\alpha\omega}\frac{\mathrm{d}u}{\mathrm{d}y}\right)\hat{\boldsymbol{y}}, \tag{67}$$

and the boundary integral

$$\Gamma'(X) = -\left[\int_0^\infty (\boldsymbol{V}'u)\cdot\hat{\boldsymbol{v}}_{\alpha\omega}\,\mathrm{e}^{-\mathrm{i}\alpha x}\,\mathrm{d}y\right]_{x=-X}^{x=X}. \tag{68}$$

The volume integral in (66) is now re-expressed in terms of h by writing the following adjoint problem:

$$\mathbf{L}(U\hat{\boldsymbol{x}}; R)(\tilde{\boldsymbol{V}}(y)\,\mathrm{e}^{-\mathrm{i}\alpha x}) + \boldsymbol{\nabla}(\tilde{P}(y)\,\mathrm{e}^{-\mathrm{i}\alpha x}) = \tilde{\boldsymbol{Q}}(y)\,\mathrm{e}^{-\mathrm{i}\alpha x}, \tag{69}$$

$$\boldsymbol{\nabla}\cdot(\tilde{\boldsymbol{V}}(y)\,\mathrm{e}^{-\mathrm{i}\alpha x}) = 0, \tag{70}$$

$$\tilde{\boldsymbol{V}} = \boldsymbol{0} \quad \text{on} \quad y = 0, Y. \tag{71}$$

This problem defines $\tilde{\boldsymbol{V}}$. Using a stream-function representation for $\tilde{\boldsymbol{V}}(y)\,\mathrm{e}^{-\mathrm{i}\alpha x}$, taking the curl of equation (69) gives an inhomogeneous adjoint Orr–Sommerfeld problem which can be solved with relative ease by numerical means.

Substituting for $\tilde{\boldsymbol{Q}}(y)$ in the volume integral in (66) with the left-hand side of (69), and making use of the Lagrange identity, we find that

$$\begin{aligned} A_1 &= -\int_{-X}^{X} \mathrm{d}x \int_0^\infty \mathrm{d}y\, \boldsymbol{V}'(x,y)\cdot(\tilde{\mathbf{L}}(\boldsymbol{V}; R)(\tilde{\boldsymbol{V}}\,\mathrm{e}^{-\mathrm{i}\alpha x}) + \boldsymbol{\nabla}(\tilde{P}\,\mathrm{e}^{-\mathrm{i}\alpha x})) + \Gamma'(X) \\ &= \int_{-X}^{X} \mathrm{d}x \int_0^\infty \mathrm{d}y\,\{(\mathbf{L}(\boldsymbol{V}; R)\,\boldsymbol{V}' + \boldsymbol{\nabla}P')\cdot\tilde{\boldsymbol{V}}\,\mathrm{e}^{-\mathrm{i}\alpha x} - \boldsymbol{\nabla}\cdot(J(S', \tilde{S}))\} + \Gamma'(X) \\ &= -\frac{1}{R}\left(\frac{\mathrm{d}U}{\mathrm{d}y}\frac{\mathrm{d}\tilde{U}}{\mathrm{d}y}\right)_{y=0}\int_{-X}^{X} \mathrm{d}x\, h(x)\,\mathrm{e}^{-\mathrm{i}\alpha x} + \Gamma(X), \end{aligned} \tag{72}$$

after substituting (6) for $J(S', \tilde{S})$, where $\tilde{S} = (\tilde{\boldsymbol{V}}, \tilde{P})\,\mathrm{e}^{-\mathrm{i}\alpha x}$. Boundary integral $\Gamma(X)$ includes $\Gamma'(X)$ plus other contributions from stations $x = \pm X$. The integral $\Gamma(X)$ represents the contribution of scattering effects in the region $|x| > X$. Assuming a local interaction zone requires that $\Gamma(X) \to 0$ as $X \to \infty$.

As X increases, $a_\pm$ approaches the amplitude of the Tollmien–Schlichting wave at stations $x = \pm X$. The boundary condition demands that there be no incoming Tollmien–Schlichting wave from upstream at order ϵ_h indicating that $a_- \to 0$. Thus the amplitude of the instability induced by the scattering of the free-stream disturbance is

$$a_+ = \Lambda\hat{h}(\alpha), \quad \text{where} \quad \hat{h}(\alpha) = \int_{-\infty}^{\infty} \mathrm{d}x\, h(x)\,\mathrm{e}^{-\mathrm{i}\alpha x} \tag{73}$$

and

$$\Lambda = -\frac{1}{R}\left(\frac{\mathrm{d}U}{\mathrm{d}y}\frac{\mathrm{d}\tilde{U}}{\mathrm{d}y} + \frac{\mathrm{d}u}{\mathrm{d}y}\frac{\mathrm{d}\tilde{u}_{\alpha\omega}}{\mathrm{d}y}\right)_{y=0}. \tag{74}$$

When solving (69)–(71) for $\tilde{\boldsymbol{V}}$, 104 Chebychev polynomials are used to construct the stream function for $\tilde{\boldsymbol{V}}$. A plot of $|\Lambda|$ as a function of $fR^{3/2}$ for various frequencies is

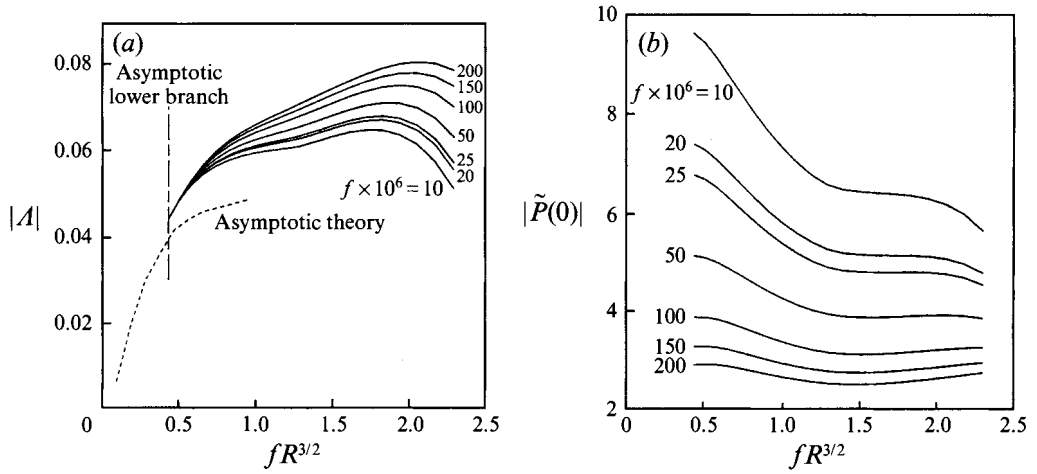

FIGURE 7. (*a*) Plot of $|A|$ as a function of $fR^{3/2}$, for various frequencies. Dashed line shows asymptotic theory (Goldstein), valid near the lower branch (chain–dash line) as $R\to\infty$. (*b*) Plot of $|\tilde{P}(0)|$ as a function of $fR^{3/2}$, for various frequencies.

shown in figure 7(*a*). The asymptotic theory of Goldstein (1985) is valid in the vicinity of, and below, the lower branch of the neutral stability curve (the asymptotic position $fR^{3/2}=0.44$ is shown as a chain–dash line) as the Reynolds number approach infinity. The asymptotic value for $|A|$ is shown as a dashed line and represents the quantity $\lambda_0^2|A(f(R/\lambda_0)^{3/2})|(2\pi)^{1/2}$, $\lambda_0=U'(0)=0.332$, where A is taken from Goldstein's figure 5. This defines the maximum streamwise fluctuations in the middle deck. The curves with lower frequencies of course have higher neutral-stability Reynolds numbers and consequently are expected to approach the asymptotic theory more closely. In fact all the curves collapse to close to the asymptotic value around $fR^{3/2}=0.44$. The maximum value of $|A|$ is taken for $fR^{3/2}\approx 2$, beyond which the value diminishes. This maximum is above the upper branch of the neutral stability curve at high frequencies, and below it at low frequencies.

Both Crouch (1992) and Choudhari & Streett (1992) calculate the efficiency factor for this problem by evaluating a residue from contour integration. The results of Crouch are in direct agreement with the present results (see his figure 3). The parameter $A_u^{(3)}$ defined by Choudhari & Streett is equal to $(1.721)^2(2\pi)^{1/2}A$.

6.2. *Variations in surface admittance and mean suction*

The surface admittance is defined as the ratio at the wall of the unsteady normal velocity to the unsteady pressure, and thus can be used to represent how the surface responds dynamically to unsteady pressures. Suppose that there are spatially uniform fluctuations $p_0 e^{-i\omega t}$ in the pressure field. If $\beta_w(x)$ is the surface admittance in the vicinity of a position a distance L from the leading edge, then the surface will respond with a normal velocity fluctuation $p_0\beta_w(x)e^{-i\omega t}$. From (34), (32), this will induce a Tollmien–Schlichting wave of amplitude

$$|\tilde{p}_{\alpha\omega}(0)|\,p_0\int_{-\infty}^{\infty}\beta_w(x)e^{-i\alpha x}\,dx. \tag{75}$$

The adjoint pressure at the wall defines the efficiency factor for the scattering of free-stream pressure fluctuations into Tollmien–Schlichting waves. Choudhari & Streett (1992) obtain the equivalent quantity from a residue calculation. It is denoted by them

as $\Lambda_u^{(2)}$ and is equal to 1.721 $(2\pi)^{1/2}\tilde{p}_{\alpha\omega}(0)$ (see figure 4). The present numerical values agree with theirs (Choudhari & Streett, figure 9*b*).

The distortion of the mean flow in the vicinity of suction holes or slots can also serve to scatter free-stream disturbances into Tollmien–Schlichting waves. Consider a velocity distribution $V_s(x)$ representing a suction/blowing distribution on the plate. The plate boundary condition $V'(x,0) = V_s(x)$ replaces that in (58). The effect of variable wall admittance has already been discussed so it is assumed that $\boldsymbol{v}' = \boldsymbol{0}$ at the plate. This replaces the wall condition in (61). It follows that the amplitude of the Tollmien–Schlichting wave is

$$\left(\tilde{P}\hat{\boldsymbol{y}} + \frac{1}{R}\frac{\mathrm{d}\tilde{U}}{\mathrm{d}y}\hat{\boldsymbol{x}}\right)\cdot\int_{-\infty}^{\infty}\mathrm{d}x\, V_s(x)\,\mathrm{e}^{-\mathrm{i}\alpha x}. \tag{76}$$

The value of $|\tilde{P}(0)|$ is plotted in figure 7(*b*), and represents the efficiency factor for scattering of acoustic waves by normal wall suction. Choudhari & Streett (1992) calculate the effect of normal blowing/suction ($V_s\cdot\hat{\boldsymbol{x}} = 0$) by a residue calculation. They name it $\Lambda_u^{(1)}$ and it is equal in value to 1.721 $(2\pi)^{1/2}\tilde{P}(0)$.

7. Conclusions

The normalized adjoint to the Tollmien–Schlichting eigensolution is shown to define the efficiency with which various types of sources will excite this characteristic boundary layer motion. The value of the adjoint velocity at a point in the flow indicates the response which will arise from an unsteady momentum source at that point. The adjoint pressure and the adjoint stream function play the same role for mass sources and vorticity sources, respectively. The response to motion at the boundary, or of the boundary, is taken into account by considering an adjoint stress vector.

The adjoint fields are easy to compute, and have a clear physical interpretation, more so than the residue expressions resulting from a traditional Fourier-inversion solution method. Mathematically, the adjoint field values are equivalent to the results of residue evaluations. The vibrating ribbon problem (Ashpis & Reshotko 1990), and the response of an inviscid wake to a point vorticity source (Huerre & Monkewitz 1985), have been explored as examples.

Investigation of the Blasius boundary layer reveals that unsteady forcing in the vicinity of the critical layer will induce the largest response of the Tollmien–Schlichting wave. The precise height depends upon frequency and Reynolds number (see figure 3*b*). Forcing in the wall-normal direction is much less effective than forcing aligned with the stream. Conversely, for motion at the boundary (or of the boundary) the response to normal motion is much stronger than streamwise motion.

Disturbances can grow by several orders of magnitude as they travel downstream in the unstable regime, particularly at lower frequencies. The relatively slow streamwise variation in the adjoint field magnitudes indicates that forcing in the vicinity of the lower branch of the neutral stability curve will induce the largest possible response.

A finite-Reynolds-number approach has been developed to describe the scattering of infinite-wavelength free-stream disturbances into Tollmien–Schlichting waves by surface roughness. The results approach the asymptotic results of Goldstein (1985) close to the lower branch, at high Reynolds number, and are in direct agreement with previous finite-Reynolds-number computations.

The author is pleased to acknowledge several helpful discussion with M. Tobak and P. A. Durbin.

REFERENCES

ACKERBERG, R. C. & PHILLIPS, J. H. 1972 The unsteady laminar boundary layer on a semi-infinite flat plate due to small fluctuations in the magnitude of the free stream velocity. *J. Fluid Mech.* **51**, 137–157.

ASHPIS, D. E. & RESHOTKO, E. 1990 The vibrating ribbon problem revisited. *J. Fluid Mech.* **213**, 531–547.

BALSA, T. F. 1988 On the receptivity of free shear layers to two-dimensional external excitation. *J. Fluid Mech.* **187**, 155–177.

BRIDGES, T. J. & MORRIS, P. J. 1987 Boundary layer stability calculations. *Phys. Fluids* A **30**, 3351–3358.

CHANDRASEKHAR, S. 1989 Adjoint differential systems in the theory of hydrodynamic stability. In *Selected Papers of S. Chandrasekhar*, vol. 4, pp. 221–228. University of Chicago Press.

CHOUDHARI, M. & STREETT, C. L. 1992 A finite Reynolds number approach for the prediction of boundary-layer receptivity in localized regions. *Phys. Fluids* A **4**, 2495–2514.

CODDINGTON, E. A. & LEVINSON, N. 1955 *Theory of Ordinary Differential Equations*. McGraw-Hill.

COURANT, R. & HILBERT, D. 1962 *Methods of Mathematical Physics*, vol. 2. Interscience.

CROUCH, J. D. 1992 Localized receptivity of boundary layers. *Phys. Fluids* A **4**, 1408–1414.

DRAZIN, P. G. & REID, W. H. 1981 *Hydrodynamic Stability*. Cambridge University Press.

ECKHAUS, W. 1965 *Studies in Non-linear Stability Theory*. Springer.

FINLAYSON, B. A. 1972 Existence of variational principles for the Navier–Stokes equation. *Phys. Fluids* **15**, 963–967.

FRIEDMAN, B. & MISHOE, L. I. 1956 Eigenfunction expansions associated with a non-self-adjoint differential equation. *Pacific J. Maths* **6**, 249–270.

FUCHS, L. 1858–1875 *Gessammelte Mathematische Werke I.* Mayer and Muller, Berlin.

GASTER, M. 1965 On the generation of spatially growing waves in a boundary layer. *J. Fluid Mech.* **22**, 433–441.

GOLDSTEIN, M. E. 1983 The evolution of Tollmien–Schlichting waves near a leading edge. *J. Fluid Mech.* **127**, 59–81.

GOLDSTEIN, M. E. 1985 Scattering of acoustic waves into Tollmien–Schlichting waves by small streamwise variations in surface geometry. *J. Fluid Mech.* **154**, 509–529.

GOLDSTEIN, M. E. & HULTGREN, L. S. 1987 A note on the generation of Tollmien–Schlichting waves by a sudden surface-curvature change. *J. Fluid Mech.* **181**, 519–525.

GOLDSTEIN, M. E., LEIB, S. J. & COWLEY, S. J. 1987 Generation of Tollmien–Schlichting waves on interactive marginally separated flows. *J. Fluid Mech.* **181**, 485–517.

GOLDSTEIN, M. E., SOCKOL, P. M. & SANZ, J. 1983 The evolution of Tollmien–Schlichting waves near a leading edge. Part 2. Numerical determination of amplitudes. *J. Fluid Mech.* **129**, 443–453.

GUSTAVSSON, L. H. 1979 Initial value problem for boundary layer flows. *Phys. Fluids.* **22**, 1602–1605.

HILL, D. C. 1992 A theoretical approach for analyzing the restabilization of wakes. *AIAA Paper* 92-0067.

HUERRE, P. & MONKEWITZ, P. A. 1985 Absolute and convective instabilities in free shear layers. *J. Fluid Mech.* **159**, 151–168.

INCE, E. L. 1944 *Ordinary Differential Equations*. Dover.

IOOSS, G. & JOSEPH, D. D. 1980 *Elementary Stability and Bifurcation Theory*. Springer.

KOZLOV, V. V. & RYZHOV, O. S. 1990 Receptivity of boundary layers: asymptotic theory and experiment. *Proc. R. Soc. Lond.* A **429**, 341–373.

LAGRANGE, J. L. 1867 *Oeuvres de Lagrange*, p. 471. Gauthier-Villars. (Originally in *Miscellanea Taurinensia*, t. III, 1762–1765.)

LING, C. H. & REYNOLDS, W. C. 1973 Non-parallel flow corrections for the stability of shear flows. *J. Fluid Mech.* **59**, 571–591.

MACARAEG, M. G., STREETT, C. L. & HUSSAINI, M. Y. 1988 A spectral collocation solution to the compressible stability eigenvalue problem. *NASA Tech. Paper* 2858.

MORSE, P. M. & FESHBACH, H. 1953 *Methods of Theoretical Physics*. McGraw-Hill.

NAYFEH, A. H. 1981 *Introduction to Perturbation Techniques*. John Wiley.

ROBERTS, P. H. 1960 Characteristic value problems posed by differential equations arising in hydrodynamics and hydromagnetics. *J. Math. Anal. Applics.* **1**, 195–214.

SALWEN, H. 1979 Expansions in spatial or temporal eigenmodes of the linearised Navier–Stokes equations. *Bull. Am. Phys. Soc.* **24**, 74.

SALWEN, H. & GROSCH, C. E. 1981 The continuous spectrum of the Orr–Sommerfeld equation. Part 2. Eigenfunction expansions. *J. Fluid Mech.* **104**, 445–465 (referred to herein as SG).

SARIC, W. S. & NAYFEH, A. H. 1975 Nonparallel stability of boundary-layer flows. *Phys. Fluids* **18**, 945–950.

SCHENSTED, I. V. 1960 Contributions to the theory of hydrodynamic stability. PhD dissertation, University of Michigan.

SCHUBAUER, G. B. & SKRAMSTAD, H. K. 1947 Laminar boundary layer oscillations and transition on a flat plate. *J. Aero. Sci.* **14**, 69–76. (Also *NACA Rep.* 909, 1948.)

TAM, C. K. W. 1978 Excitation of instability waves in a two-dimensional shear layer by sound. *J. Fluid Mech.* **89**, 357–371.

TITCHMARSH, E. C. 1962 *Eigenfunction Expansions Associated with Second-order Differential Equations*, 2nd edn. Clarendon.

VUJANOVIC, B. D. & JONES, S. E. 1989 *Variational Methods in Non-conservative Phenomena*. Academic.

ZHIGULEV, V. N. & FEDOROV, A. V. 1987 Boundary layer receptivity to acoustic disturbance. *Zh. Prikl. Mekh. Tekh. Fiz.* no. 1, 30–37.

ZHIGULEV, V. N., SIDORENKO, N. V. & TUMIN, A. M. 1980 Generation of instability waves in a boundary layer by external turbulence. *Zh. Prikl. Mekh. Tekh. Fiz.* no. 6, 43–49.